Article:
Rajani, K, Parrish, C, Kottke, T et al. (2016) Combination therapy with reovirus and anti-PD-1 blockade controls tumor growth through innate and adaptive immune responses. Molecular Therapy, 24 (1). pp. 166-174. ISSN: 1525-0016

https://doi.org/10.1038/mt.2015.156

Accepted Article Preview: Published ahead of advance online publication

Combination therapy with reovirus and anti-PD-1 blockade controls tumor growth through innate and adaptive immune responses

Karishma Rajani, Christopher Parrish, Timothy Kottke, Jill Thompson, Shane Zaidi, Liz Ilett, Kevin G. Shim, Rosa-Maria Diaz, Hardev Pandha, Kevin Harrington, Matt Coffey, Alan Melcher, and Richard Vile

Cite this article as: Karishma Rajani, Christopher Parrish, Timothy Kottke, Jill Thompson, Shane Zaidi, Liz Ilett, Kevin G. Shim, Rosa-Maria Diaz, Hardev Pandha, Kevin Harrington, Matt Coffey, Alan Melcher, and Richard Vile, Combination therapy with reovirus and anti-PD-1 blockade controls tumor growth through innate and adaptive immune responses, *Molecular Therapy* accepted article preview online 27 August 2015; doi:10.1038/mt.2015.156

Received 20 May 2015; accepted 23 August 2015; Accepted article preview online 27 August 2015

Combination therapy with reovirus and anti-PD-1 blockade controls tumor growth through innate and adaptive immune responses.

Karishma Rajani[1*], Christopher Parrish[5*], Timothy Kottke[1], Jill Thompson[1], Shane Zaidi, Liz Ilett, Kevin G. Shim[1], Rosa-Maria Diaz[1], Hardev Pandha[2], Kevin Harrington[3], Matt Coffey[4], Alan Melcher[5], and Richard Vile[1,6]

[1]Department of Molecular Medicine, [2]University of Surrey, Guildford, UK, [3]The Institute of Cancer Research, 237 Fulham Road, London, SW3, [4]Oncolytics Biotech Incorporated, Calgary, Canada, [5]Cancer Research UK Clinical Centre, St. James' University Hospital, Leeds, UK; [6]Department of Immunology, Mayo Clinic, Rochester, MN 55905

Running title: Reovirus and anti-PD-1 control tumor growth

Financial Support: The Richard M. Schulze Family Foundation, the Mayo Foundation, Cancer Research UK, the National Institute of Health (R01CA107082, R01CA130878, R01CA132734) and a grant from Terry and Judith Paul. This work was funded in part by a grant received from Oncolytics Biotech Incorporated.

Correspondence should be addressed to R.V. (vile.richard@mayo.edu) / Mayo Clinic / Gugg 18 / 200 First Street SW / Rochester, MN 55905 / Phone: 507-284-3178 / FAX: 507-266-2122.

* These authors contributed equally to this work.

Keywords: reovirus, anti-PD-1, immunotherapy, NK cells, innate and adaptive response

Conflict of Interest: This work was funded in part by a grant received from Oncolytics Biotech Incorporated.

ABSTRACT

Oncolytic reovirus can be delivered both systemically and intratumorally, in both pre-clinical models and in early phase clinical trials. Reovirus has direct oncolytic activity against a variety of tumor types and anti-tumor activity is directly associated with immune activation by virus replication in tumors. Immune mechanisms of therapy include both innate immune activation against virally infected tumor cells, and the generation of adaptive anti-tumor immune responses as a result of *in vivo* priming against tumor-associated antigens. We tested the combination of local oncolytic reovirus therapy with systemic immune checkpoint inhibition. We show that treatment of subcutaneous B16 melanomas with a combination of intravenous (i.v.) anti-PD-1 antibody and intratumoral (i.t.) reovirus significantly enhanced survival of mice compared to i.t. reovirus ($p<0.01$) or anti-PD-1 therapy alone. *In vitro* immune analysis demonstrated that checkpoint inhibition improved the ability of NK cells to kill reovirus-infected tumor cells, reduced T_{reg} activity, and increased the adaptive $CD8^+$ T cell dependent anti-tumor T cell response. PD-1 blockade also enhanced the anti-viral immune response but through effector mechanisms which overlapped with, but also differed from those affecting the antitumor response. Therefore, combination with checkpoint inhibition represents a readily translatable next step in the clinical development of reovirus viroimmunotherapy.

INTRODUCTION

Reovirus is a double stranded RNA virus with oncolytic activity in a variety of cancer cell types [1]. Although reovirus has been demonstrated to replicate independently of the Ras-EGFR pathway in certain cells [2], direct oncolysis can occur as a result of defective anti-viral PKR signalling in many tumor cells, leading to efficient viral replication and preferential tumor cell lysis. We, and others, have also shown that the anti-tumor efficacy of reovirus depends upon a potent anti-tumor immune response through activating dendritic cells (DCs) to stimulate both NK cell and T cell mediated cytotoxicity [3-8]. Following on from these pre-clinical studies, safety of reovirus serotype 3 Dearing strain (Oncolytics, Reolysin) alone, or in combination with other therapies, has been demonstrated in several phase I/II clinical trials [9-16]

During normal cellular immune homeostasis, several immune checkpoint ligand-receptor interactions act as negative regulators of T cell responses to regulate autoimmunity and prevent damage to healthy tissues [17]. Programmed cell death-1 (PD-1) is a checkpoint receptor expressed on T, B cells, and monocytes [18, 19], binding of which to its ligands PD-L1, PD-L2 inhibits T cell activation [20, 21]. In this way, expanding T cell responses to, for example, viral infections or tumor development, are restricted and dampened. In this respect, it is now clear that expression of molecules such as PD-L1 is one of the many mechanisms which tumors employ to inhibit developing anti-tumor T cell responses [22-24] and evade immune surveillance [25]. As a result, antibodies blocking the interaction of immune checkpoint molecules expressed on the surface of tumor cells with their ligands on immune cells, have been shown to ameliorate such tumor-induced immune suppression and enhance anti-tumor responses [26, 27]. Clinical trials have now shown the efficacy of anti-checkpoint inhibitor antibodies for the treatment of cancer patients [28-30] and FDA approval has recently been granted for their clinical use.

Since oncolytic viruses activate anti-tumor immune effector cells, either innate and/or adaptive [31, 32], their use in combination with immune checkpoint inhibitors is attractive to boost developing T cell responses against systemic tumor [33-35]. However, checkpoint inhibitors used in the context of oncolytic virotherapy will have the added effect of de-suppressing anti-viral T cell responses, which normally act to restrict viral replication. Immune responses against the virus which prevent further replication are generally regarded as detrimental to the efficacy of the directly oncolytic component of the virotherapy [31, 36]. In such instances, de-suppression by checkpoint inhibition would be predicted to reduce overall therapy. In contrast, antitumor therapy may actually benefit from those immune responses which contribute to tumor clearance [7, 37-39], in which case immune checkpoint inhibition may add to, or synergise with, direct oncolytic virotherapy in clearing tumor cells. Finally, any differential effects of immune checkpoint inhibitors on both innate, and adaptive, immune effectors, to both virus and tumor, will also impact on overall treatment efficacy. Thus, although de-suppression of local acting, innate immune responses to virus infection may act to restrict viral oncolysis, it may, conversely, increase local immune-mediated tumor clearance. Similarly, immune checkpoint inhibition of slower developing, adaptive antitumor T cell responses would be expected to contribute to improved overall therapy, whilst preventing the suppression of anti-viral T cell responses may lead to decreased efficacy of repeated treatments. Therefore, the overall therapeutic effects of immune checkpoint inhibitor therapy, in combination with oncolytic viroimmunotherapy are likely to be dependent upon multiple factors including the nature of the virus, the checkpoint inhibitor, the tumor type and pragmatic issues such as the relative timing of administration of the agents.

Therefore, in the current study, we investigated whether it would be possible to combine systemic checkpoint inhibitor therapy with local viroimmunotherapy using oncolytic reovirus in

our pre-clinical model of subcutaneous (s.c.) B16 melanoma. We show here that combining intravenous (i.v.) anti-PD-1 antibody with intra-tumoral (i.t.) reovirus, significantly enhanced survival compared to either therapy alone. Successful combination therapy was associated with an enhanced ability of natural killer (NK) cells to recognize, and kill, reovirus-infected target tumor cells, an anti PD-1 antibody-mediated reduction in regulatory T cell (T_{reg}) activity in reovirus-treated mice, and an increased adaptive CD8+ antitumor T cell response. Our data show that combination with checkpoint inhibition represents a readily translatable next step in the clinical development of reovirus viroimmunotherapy.

RESULTS

PD-1 blockade with i.t. reovirus prolongs survival. We used a regimen of treatment of s.c. B16 tumors in C57Bl/6 immune competent mice with i.t. reovirus [5] such that virus delayed tumor growth but had no significant effect on survival compared to PBS-treated mice (**Fig.1**). In this model, systemic treatment with anti-PD-1 antibody also gave no survival benefit (**Fig.1**). In contrast, when anti-PD-1 antibody was administered starting 7 days after the first i.t. virus treatment, combining both treatments significantly prolonged survival of mice ($p< 0.001$ compared to i.t. reovirus), and cured ~40% of mice. Cured mice were tumor free for >100 days.

PD-1 blockade and reovirus together augments the IFN-γ response against melanoma tumor-associated antigens. An IFN-γ memory recall response to B16 tumor cell lysates was detected from pooled splenocytes and lymph node (splenocytes/LN) cells of mice treated with i.t. reovirus, but not from mice treated with i.t. PBS ($p=0.035$) (**Fig.2a**), confirming our previous reports that oncolytic reovirus effectively primes antitumor T cell responses [4, 8]. Consistent with the increased therapy associated with combination with anti-PD-1 treatment (**Fig.1**), splenocytes/LN from mice treated with the combination of reovirus and anti-PD-1 generated significantly higher levels of IFN-γ in response to B16 tumor lysates compared to reovirus alone ($p=0.017$) (**Fig.2a**). <20ng/ml of IFN-γ were secreted in response to lysates of the

prostate (non-melanoma) TC2 cell line, indicating that these T cell responses were tumor specific (data not shown and **Fig.5**). With respect to the specificity of these anti-B16 responses induced by i.t. reovirus, splenocytes/LN cells from both reovirus/PBS and reovirus/anti-PD-1 groups (mice 4&5; 8&9 of **Fig.2a**) contained T cells specific for the murine (but not human) gp100, TYRP-1 and TYRP-2 melanoma antigens. However, as for the B16 lysates, addition of anti-PD-1 treatment to i.t. reovirus significantly enhanced the magnitude of the anti-melanoma responses (**Fig.2b**). These data show that addition of PD-1 checkpoint inhibition to reovirus therapy augments the *in vivo* IFN-γ response against melanoma tumor-associated antigens.

PD-1 blockade augments reovirus-induced NK cell activation and killing. We have previously shown that both tumor[4, 6-8], and immune[3], cell infection with reovirus elicits NK cell mediated innate immune responses. Therefore, we investigated the impact of anti-PD-1 treatment on NK cell recognition of reovirus-infected tumor cells. Neither B16 tumor cells, nor cultures enriched for purified splenic NK cells, alone produced high levels of tumor necrosis factor alpha (TNF-α). However, co-culture of both together led to a significant increase in TNF-α production ($p<0.0001$), which was significantly further enhanced when the B16 cells were pre-infected with reovirus ($p<0.0001$, 2-way ANOVA) (**Fig.3a**). Addition of anti-PD-1 antibody significantly increased TNF-α production by NK-enriched cultures in the presence of reovirus pre-infection of B16 targets compared to co-cultures treated with an isotype control ($p<0.0001$), but did not alter NK recognition of uninfected B16 targets (**Fig.3a**). *In vitro* PD-L1 blockade had a much smaller, although still significant, effect on enhancing NK recognition of reovirus-infected B16 cells ($p<0.0001$) (**Fig.3a**).

Although co-culture of NK-enriched cultures with reovirus-infected tumor cells did not significantly reduce reovirus titers produced by the B16 cells (**Fig.3b**), addition of anti-PD-1 antibody to these co-cultures resulted in a significant decrease in reovirus titers ($p=0.037$)

(**Fig.3b**), presumably reflecting the decreased tumor cell numbers available for reovirus replication (**Fig.3c**). Neither anti-PD-L1, nor isotype control IgG, decreased reovirus titers compared to co-cultures with NK cells alone (**Fig.3b**). The addition of anti-PD-1, anti-PD-L1 or isotype control antibodies to uninfected B16-NK co-cultures had no effect on tumor cell survival (**Fig.3c**). Consistent with additional virus-mediated killing of B16 cells, addition of reovirus to B16/NK co-cultures reduced viable cell numbers (**Fig.3c**). However, the addition of anti-PD-1 antibody to reovirus-infected B16 /NK cell co-cultures significantly augmented NK cell-mediated tumor killing compared to the addition of no antibody ($p=0.012$), a control IgG or anti-PD-L1 antibody (**Fig.3c**). Although PD-1 expression could be detected at low levels on resting CD4 cells, minimal levels of PD-1 were detectable on the resting CD8 T cells and NK cells used in these experiments (**Fig.3D-F**). Therefore, the anti-PD-1-augmented NK activation of tumor cell killing by reovirus infection observed in these NK-enriched populations *in vitro* (**Fig.3A-C**) was most likely occuring through indirect mechanisms. Consistent with this, the NK-enriched cultures contained a signficant number of non-NK cells which expressed high levels of PD-1 (**Fig.3G**). Taken together, these data suggest a model in which anti-PD-1 treatment alleviated suppression of NK mediated anti tumor activity exerted by a population of PD-1^{Hi} innate immune cells, which secrete factors which directly activate NK cell mediated killing of tumor cells in a reovirus sensitive manner.

Reovirus in combination with NK cells affects the levels of PD-L1 on tumors. The B16 cells used in this study expressed high levels of PD-L1 (**Fig.4a**) but these were not significantly changed upon infection by reovirus at the indicated MOI (**Fig.4a**). Similarly, co-culture of B16 cells with NK cells *in vitro* did not alter the high levels of PD-L1 expressed by the tumor cells (**Fig.4b**). Pre-infection of the tumor cells with reovirus, followed by co-culture with NK cells, led to a small increase in PD-L1 levels on the B16 cells (**Fig.4b**). PD-L1 levels on NK cells were not altered by reovirus infection of B16 cells prior to co-culture (**Fig.4c**). Taken together, these

data suggest that the therapeutic effects of anti-PD-1 *in vivo* were not due to direct effects on PD-L1 expression as a result of tumor cell infection by reovirus but mediated by NK cells via enhanced recognition of reovirus infected tumor cells.

*PD-1 blockade ameliorates T_{reg} suppression***.** As before, splenocyte/LN cells from mice treated with reovirus/anti-PD-1 (**Fig.2a**) had stronger memory recall responses against B16 tumor cell lysates than did splenocytes/LN cells from mice treated with reovirus/PBS (**Fig.2a** and **Fig.5a**). Depletion of CD8+ T cells from these splenocyte/LN cultures almost completely eradicated IFN-γ production in response to B16 tumor lysates, irrespective of the treatment group (**Fig.5a**). Conversely, T_{reg} depletion from the splenocyte/LN cultures of mice treated with i.t. reovirus alone significantly augmented IFN-γ production in response to re-stimulation with B16 lysates (**Fig.5a**). However, T_{reg} depletion from the splenocyte/LN cultures from mice treated with i.t reovirus and i.v. anti-PD-1 did not alter the already increased levels of IFN-γ production in response to B16 tumor lysates (**Fig.5a**). These data suggest that a CD8+ Th1 antitumor T cell response induced by i.t. reovirus treatment is suppressed by T_{reg} and that *in vivo* treatment with anti-PD-1 antibody acts to abrogate T_{reg} activity.

Differential mechanisms of checkpoint inhibition of antitumor and antiviral responses. Splenocyte/LN cells from treated mice did not have detectable (<20ng/ml IFN-γ) recall responses to the prostate cancer TC2, non-melanoma cell line, indicating that the Th1 response induced by i.t. reovirus (**Figs.2&5a**) was tumor specific (data not shown). Therefore, to assess the effects of anti-PD-1 therapy on the antiviral response, the recall response to reovirus-infected TC2 cells was measured. Anti-reo IFN-γ production from splenocyte/LN cells from reovirus/anti-PD-1 treated mice was significantly augmented compared to mice treated with i.t. reovirus alone ($p=0.031$) (**Fig.5b**). As for the antitumor response, the anti-reovirus T cell response was significantly ($p< 0.0001$) reduced upon depletion of CD8+ T cells from the splenocyte/LN cultures irrespective of the treatment (**Fig.5c**). However, unlike the antitumor

response (**Fig.5a**), depletion of CD8+ T cells from splenocyte/LN cultures did not completely eradicate IFN-γ production in response to reovirus, suggesting that the anti-reovirus response was also contributed by a non-CD8+ T cell component (**Fig.5c**). Also in contrast to the antitumor Th1 response (re-stimulation with B16 lysates, **Fig.5a**), depletion of T_{reg} did significantly enhance IFN-γ production from splenocyte/LN cultures of mice treated with i.t. reovirus and anti-PD-1 ($p< 0.0001$) (**Fig.5c**). Measurement of tumor infiltrating immune subsets from tumors of mice treated with reovirus alone, or reovirus with anti-PD-1, at a single time point, (day 22 after tumor challenge, 3 i.t. reo and 4 doses of i.v. anti-PD1 or isotype antibody), did not reveal any significant differences in the levels of tumor infiltrating CD4, CD8, NK, or Treg cells between groups (**Fig.5D**). Experiments are underway to investigate whether this lack of difference reflects the fact that anti-PD-1 treatment affects qualitative, rather than quantitative, aspects of tumor infiltrating cell types or whether significant changes occur at different time points in the treatment schedule.

Both innate and adaptive immunity contribute to the in vivo efficacy of reovirus with PD-1 blockade. Our *in vitro* studies suggested that the improved therapy conferred by i.v. anti-PD-1 antibody (**Fig.1**) was mediated through effects on both NK cells (**Fig.3**) and CD8+ T cells, (**Fig.5**). Consistent with these data, depletion of either NK ($P= 0.0004$), or CD8+ T ($p=0.0024$), cells significantly reduced the antitumor efficacy of i.t. reovirus with i.v. anti-PD-1 therapy compared to non-depleted mice (**Fig.6**). However, depletion of CD4+ T cells had no significant effect on antitumor therapy (**Fig.6**).

DISCUSSION

We show here, for the first time to our knowledge, that reovirus oncolytic viroimmunotherapy can be successfully combined with immune checkpoint inhibitor therapy. Our data complement previous reports in which other oncolytic viruses have been used in tandem with immune checkpoint inhibitors [33-35]. Cumulatively, these data sets confirm that oncolytic

virotherapy can be regarded as a form of immunotherapy and that strategies aimed at enhancing the immune based component of this approach are likely to enhance its therapeutic efficacy [5-7].

Consistent with our previous studies on reovirus oncolysis in the B16 model [4, 6-8, 40] i.t. injection of established tumors primed tumor-specific Th1 T cell responses against both tumor cells (**Fig.2a**), and against defined melanoma-associated antigens (**Fig.2b**). These results indicated that both direct oncolysis, as well as the immune based activation that accompanies it [4, 6, 8, 40], provides sufficient immune activation to break tolerance to self -antigens expressed by the tumor (**Fig.2b**). Therefore, we hypothesized that the immune stimulating, T cell priming activity associated with direct oncolysis by reovirus could be effectively combined with immune checkpoint inhibition. In this way, the weak antitumor T cell responses generated by the immunostimulatory activity of the virus would be enhanced by blockade of negative regulatory signals to the activated self-responsive T cells. Consistent with this hypothesis, direct i.t. injection of reovirus, followed 7 days later by multiple systemic administrations of anti-PD-1 antibody, significantly improved on the therapy associated with either virus, or anti-PD-1 antibody, alone (**Fig.1**).

We initially showed a significant increase in the IFN-γ response to B16 tumor in splenocytes/lymph node cells from mice treated with reovirus and anti-PD-1 compared to reovirus alone (**Fig.2**). To dissect the cellular basis of this response in more detail, we proceeded to show that the response is mediated by NK cells (**Figs.3&6**), Treg (**Fig.5**) and CD8+ T cells (**Figs.5&6**) but not significantly by CD4+ T cells (**Fig.6**). The majority of data suggests that immune checkpoint inhibitor therapy acts through modulating activation of T lymphocytes [29, 30, 41, 42]. However, based on our previous studies showing NK-mediated recognition of reovirus-infected tumor cells [3, 4], we investigated the effects of anti-PD-1 on NK cell activation in the context of reovirus oncolysis. As we have reported previously, NK

cells were activated by B16 cells *in vitro*, but this was significantly enhanced by reovirus infection (**Fig.3a**). In the presence of anti-PD-1 antibody, NK cell activation by reovirus infection was significantly enhanced as evidenced by TNF-α secretion (**Fig.3a**) and target cell killing (**Fig.3c**). Interestingly, at least in the context of this *in vitro* assay, anti-PD-1 antibody decreased the viral titers associated with NK/B16-reovirus infection (**Fig.3b**), suggesting that the increased immune based killing associated with NK/anti-PD-1 recognition of reovirus-infected tumor cells may be more important than direct oncolysis effects. Taken together with the *in vivo* confirmation of a strict dependence upon NK cells for reovirus/anti-PD-1 therapy (**Fig.6**), overall our data show that NK activation by, and killing of, B16 tumor cells is significantly enhanced by blockade of PD-1. However, we were unable to detect PD-1 expression on NK cells from splenocytes/lymph node cells from C57Bl/6 mice (**Fig.3**), although these cells had high levels of PD-L1 (**Fig.4**). Therefore, it seems probable that the NK-dependence of the *in vitro* (**Fig.3**) and *in vivo* (**Fig.6**) effects of anti-PD-1 treatment with reovirus infection were mediated through an indirect mechanism of NK activation. We are currently testing the hypothesis that reovirus infection of tumor ($PD\text{-}1^{-ve}$, $PD\text{-}L1^{Hi}$), and/or innate immune effectors ($PD\text{-}1^{Hi}$), leads to the secretion of cytokines which directly activate NK cell mediated killing of tumor cells. In this model, anti-PD-1 treatment would alleviate suppression of NK-activating cytokine secretion from $PD\text{-}1^{Hi}$ innate immune cells - which is exerted through PD-L1 expression by the B16 tumor, NK or other cell types – and which is enhanced by reovirus infection. This model is consistent with our previous demonstration that reovirus infection of innate immune cells, such as dendritic cells, induces cytokines which activate NK killing of tumor [3]. It is also consistent with the results of **Fig.3** which show that NK cells both recognise (through TNF-α secretion, **Fig.3A**), and kill (**Fig.3C**), B16 target cells, even in the absence of reovirus infection. Hence, enhanced activation of NK cells through indirect mechansims (such as infection/activation of DC by reovirus) would further add to tumor

cell clearance *in vivo*. In this respect, it is interesting that blockade of PD-L1 was less effective at activating NK cell recognition/killing of reovirus-infected B16 cells than blockade of PD-1 (**Fig.3**). This may be due to technical reasons related to the anti-PD-L1 antibody used in our studies here, to the fact that other ligands for PD-1 may be recognized in the context of PD-1^{Hi} immune cells which mediate NK tumor cell killing, or that PD-1 signaling on innate immune effector cells may transmit suppressive signals even in the absence of PD-L1 ligation. Therefore, taken together, the *in vivo* mechanisms by which i.t. reovirus leads to anti-PD-1 augmented therapy are likely to be pleiotropic, involving both innate and adaptive immune effector mechanisms (**Figs. 2,3,5&6**).

Reovirus infection alone did not significantly alter the levels of PD-L1 on B16 tumor cells (**Fig.4a**), but addition of NK cells to reovirus infected B16 cells increased PD-L1 on the tumor cells (**Fig 4b**). Therefore, our *in vitro* data suggest that the therapeutic effects of i.t. reovirus with systemic anti-PD-1 antibody treatment *in vivo* probably did not derive from direct effects on levels of expression of PD-L1, or PD-1, induced by reovirus infection of the tumor cells. Therefore, we hypothesise that the *in vivo* therapy derived from the immune mediated sequelae of reovirus infection of tumors – namely tumor cell killing, antigen release, cytokine secretion, enhanced recognition via NK cells, and T cell priming. In this scenario, anti PD-1 antibody would act upon immune effector cells activated by this immune priming to de-suppress the developing antitumor response as seen in **Figs.1&6.** Experiments are currently underway to dissect the immune cell targets for anti-PD-1 activity *in vivo* (such as CD8+ T cells, NK cells, T_{reg}) using knockouts, immune cell depletions and flow cytometry.

In vitro cultures of splenocytes/LN cells from treated mice showed that the anti-PD-1-mediated enhancement of T cell responses against melanoma-associated antigens (**Fig.2**) was almost entirely dependent upon CD8+ T cells (**Fig.5a**), a result that was also confirmed *in vivo* (**Fig.6**). As predicted, *in vivo* blockade of PD-1 also significantly enhanced the Th1 anti-reovirus T cell

response (**Fig.5b**). However, **Fig.5c** shows that additional immune effectors contributed to the virus specific Th1 response, since *in vitro* depletion of CD8+ T cells did not completely abolish anti-reovirus IFN-γ secretion. It seems likely that NK cell mediated IFN-γ secretion may contribute, in part at least, to the anti-reovirus responses seen in these splenocyte/LN cultures given the role of NK cells shown in **Fig.3**.

Just as depletion of CD8+ T cells abolished the antitumor Th1 response induced by i.t. reovirus alone (**Fig.5a**), so *in vitro* depletion of T_{reg} dramatically increased it (**Fig.5a**). These *in vitro* data correlate closely with our previous *in vivo* data, which showed that i.t. reovirus is associated with induction of a strong T_{reg} response, which can be suppressed by antibody-mediated depletion of T_{reg}, or by treatment with cyclophosphamide [5]. Interestingly, the *in vitro* antitumor Th1 response was not further enhanced by depletion of T_{reg} from splenocyte/LN cell cultures from mice treated with i.t. reovirus and anti-PD-1 - suggesting that *in vivo* blockade of PD-1 closely mimicked an abrogation of T_{reg} activity. Although outside of the scope of the present study, we are currently investigating whether, and how, blockade of PD-1 affects T_{reg} numbers, activity or both.

In contrast to the results with the antitumor Th1 response, the anti-reovirus Th1 response was only moderately increased by *in vitro* depletion of T_{reg} (**Fig.5c**). Moreover, the anti-PD-1-mediated enhancement of the antivirus Th1 response (**Fig.5b**) was further enhanced by *in vitro* depletion of T_{reg} (**Fig.5c**). These data suggest that blockade of PD-1 does not completely mimic T_{reg} depletion/abrogation in the context of the antivirus (**Fig.5c**), as opposed to the antitumor (**Fig.5a**), response. Taken together, our data show that PD-1 blockade enhanced both tumor-specific, and viral-specific, immune responses, but may be acting through different immune effectors including CD8+ T cells, NK cells and T_{reg}.

Overall, our *in vivo* data show that tumor clearance by the combination of local oncolysis and systemic immune checkpoint inhibition absolutely depended upon immune effectors (NK,

CD8+ T cells, **Fig.6**) and that the regimen tested here led to significant synergy between the two therapies. However, the use of immune checkpoint inhibitors in the context of oncolytic virotherapy poses several possibly conflicting questions regarding its predicted therapeutic efficacy. Thus, whilst de-repressing an antitumor, adaptive T cell immune response is likely to be beneficial to tumor clearance, de-suppressing antiviral responses (innate or adaptive), which normally act to restrict viral spread, may limit further replication which could be detrimental to the efficacy of the directly oncolytic component of the virotherapy [31, 36]. Conversely, antitumor therapy may benefit from augmenting immune responses, even against the virus, which contribute to tumor clearance [7, 32, 37, 39]. Therefore, it is clear that the differential effects of immune checkpoint inhibitors on both innate, and adaptive, immune effectors, to both virus and tumor, need to be understood to allow for optimal utilization of these agents in combination with oncolytic virotherapy. Our data here clearly show that the effectors and mechanisms of the antitumor, and antiviral, Th1 responses both share some components but also differ in some significant respects. Therefore, it will be important to optimize several factors, which may play both complementary, and/or opposing, roles in the success of this combination therapy. In particular, the relative timing of virus and checkpoint inhibition may be crucial. Here, we started anti-PD-1 blockade 7 days after the first virus administration. The rationale of this was to minimize augmenting the anti viral response whilst virus injections were still being performed, thereby maximizing the ability of the virus to spread within the tumor. In the regimen of **Fig.1**, the last reovirus injection was only 2 days before the first systemic treatment with anti-PD-1. Therefore, we believe that appreciable levels of intra-tumoral reovirus would likely still be present to activate NK cell mediated tumor killing, through mechanisms which would be augmented by anti-PD-1 as shown in **Fig.3**. In addition, this timing was designed to prevent T cell inactivation as the antitumor immune response was developing (5-7 days after the initial T cell priming activity of i.t. virus injection (**Fig.2b**).

Therefore, the overall therapeutic effects of immune checkpoint inhibitor therapy, in combination with oncolytic viroimmunotherapy, are likely to be dependent upon multiple factors including the nature of the virus, the particular checkpoint inhibitor, the tumor type and pragmatic issues such as the relative timing of administration of the agents.

In summary, we show here that oncolytic reovirus therapy can be effectively combined with immune checkpoint inhibitor therapy. Blockade of PD-1 significantly enhanced the CD8+ T cell Th1 antitumor response primed by intratumoral reovirus injection and also enhanced NK cell recognition of reovirus infected tumor cells. Treatment with anti-PD-1 mimicked abrogation of T_{reg} suppression of the antitumor T cell response. PD-1 blockade also enhanced the antivirus Th1 response but not through exactly the same effector mechanisms as for the antitumor response. Therefore, combination with checkpoint inhibition represents a readily translatable next step in the clinical development of reovirus viroimmunotherapy, and careful dissection of the immune mechanisms operating in both antitumor and antiviral immune responses will help to optimize its use.

Materials and Methods

Cell lines. Murine B16 cells (American Type Culture Collection, Manassas, Va.) were grown in Dulbecco's Modified Eagle's Medium (DMEM; Life Technologies, Carlsbad,CA) supplemented with 10% (v/v) fetal calf serum (FCS; Life Technologies) and L-glutamine (Life Technologies, Carlsbad, CA).

Reovirus. Reovirus Type 3 Dearing strain was provided by Oncolytics Biotech, Inc., and stored in the dark at neat concentrations in PBS at 4℃ (maximum 3 months) or at –80℃ (long-term storage). Stock titers were determined by standard plaque assays on L929 cells.

***In vivo* studies.** All procedures were approved by the Mayo Foundation Institutional Animal Care and Use Committee. C57BL/6 mice (Thy 1.2^+) were purchased from The Jackson Laboratory (Bar Harbor, ME) at 6-8 weeks of age. To establish subcutaneous (SC) tumors,

$5x10^5$ B16-tk tumor cells in 100µl of PBS were injected into the flanks of C57BL/6 mice (7-8 mice per treatment group unless stated otherwise). Seven days later, mice were treated intra-tumorally (i.t) with PBS, or reovirus at $7x10^8$/50µl with one dose per day on alternate days, for a total of three separate doses. This was followed by intravenous (i.v.) treatments with anti-PD-1 antibody (BioXcell, West Lebanon, NH) or isotype control antibody (0.25mg/mouse) at times as described in each experiment. Tumor sizes were measured three times weekly using calipers and were euthanized when tumor size was approximately 1 cm in two perpendicular directions. For *in vivo* flow cytometry experiments, mice with established tumors were treated with 3 doses of reovirus at $7x10^8$/50µl. After four doses of IV treatment with anti-PD-1 antibody or isotype antibody, tumors were harvested, stained for immune markers and analyzed by flow cytometry (see below).

***In vitro* splenic re-stimulation of splenocytes/lymph nodes and enzyme-linked immunosorbent assay (ELISA) for IFN-γ/TNF-α.** Spleen and lymph nodes (S/LN) were immediately excised from euthanized mice and dissociated *in vitro* to achieve single-cell suspensions. Red blood cells were lysed with ACK lysis buffer for 2 minutes as described above. Cells were re-suspended at $1x10^6$ cells/mL in Iscove's Modified Dulbecco's Medium (IMDM; Gibco, Grand Island, NY) + 5% FBS + 1% Pen-Strep + 40 µM 2-ME. Supernatants were harvested from $1x10^6$ LN/S previously stimulated with virus stocks as described in the text, with synthetic H-2K^b–restricted peptides murine TRP-$2_{180-188}$ SVYDFFVWL, murine TRP-$1_{222-229}$ TAYRYHLL, human gp$100_{25–33}$ (hgp100), KVPRNQDWL, and murine gp100 (mgp100) EGSRNQDWL and/or with freeze thaw lysates from tumor cells alone or tumor cells infected with reovirus in triplicate, every 24h for 3 days. Cell-free supernatants were collected 48 hours later and tested by ELISA for murine IFN-γ (BD Biosciences, San Jose, CA) or murine TNF-α (BD Biosciences, San Jose, CA). The peptides were synthesized at Mayo Foundation Core Facility (Rochester, MN).

***In vitro* cytokine secretion, cell killing and viral titer determination.** 10^4 B16tk cells were seeded in media containing anti-PD-1 antibody (100 ng/ml) or anti-PD-L1 antibody (Biox Cell, West Lebanon, NH) or isotype-control (Chrome Pure anti-Rabbit IgG, Jackson Laboratories, Farmington, CT) and infected with reovirus at MOI 0.1. Forty eight hours post-infection, cells were co-incubated with isolated whole S/LN or S/LN enriched with NK cells (see below) derived from tumor-naïve C57BL/6 mice (E:T: 10:1). Forty eight or 72 hours post-incubation, supernatants were harvested and analyzed for cytokine secretion using ELISA and viral titers were determined by standard plaque assays on L929 cells. The number of viable cells were counted using trypan blue staining respectively.

Flow cytometry. For *in vivo* analysis of resting immune cells, spleens were harvested from C57Bl/6 mice. Splenocytes were stained with CD3-FITC, CD4-Percp, CD8- PE (eBioscience, San Diego, CA), PD1-Pe/Cy7 and PD-L1-APC (Biolegend,San Diego, CA) or for CD3-FITC, NK1.1-PE (eBioscience San Diego,CA) and PD1-Pe/Cy7, PD-L1-APC. Enriched NK cells obtained from *in vitro* cell fractionation (see below) were stained with CD3-FITC, NK1.1-PE, PD1-Pe/Cy7, PD-L1-APC to determine enrichment for NK cells from CD3+ cells.

For **Fig.4**, B16 cells were infected with reovirus at MOI= 0.1. Forty-eight hours postinfection, cells were co-incubated with NK cells isolated using Miltenyl Kit (as described above) in the absence or presence of anti-PD-1 antibody. Forty-eight post incubation, the supernatants were harvested, spin at 1200 rpm for 4 minutes. The pelleted cells were stained with CD3-FITC, CD45-PerCP (both from BD Bioscience San Diego,CA), NK1.1-PE (eBioscience San Diego,CA) and PD-L1-APC (Biolegend, San Diego, CA). Similarly, the tumor cells were also stained for CD45-PerCP (BD Bioscience San Diego,CA) and PD-L1-APC (Biolegend, San Diego,CA) expression. To determine tumor infiltrating immune cells, tumors from mice were stained with CD45-PerCP, CD8-PE. All cells were stained with antibodies with appropriate

isotype controls for 30 minutes and fixed using 4% paraformaldehyde. For T_{regs} staining, cells were stained extracellularly with CD45-Percp, CD4-FITC, CD25-Pe/Cy7, then fixed and permeabilized for intracellular staining for Foxp3-PE (eBioscience San Diego,CA) using the mouse T regulatory staining kit from eBioscience according to the manufacturer's instructions. Flow cytometry analysis was carried out by Mayo Microscopy and Cell Analysis core and data were analyzed using FlowJo software.

***In vitro* cell fractionation.** NK cells were purified/depleted from Splenocytes/LN of C57Bl/6 naïve mice using magnetic sorting with the NK Cell Isolation Kit II microbeads (Miltenyi Biotec, Auburn, CA). $CD8^+$ T cells were isolated using the MACS CD8a (Ly-2) microbead magnetic cell sorting system (Miltenyi Biotec, Auburn, CA) as per the manufacturer's instructions. T_{reg} cells were isolated from the combined spleens and lymph nodes of treated mice using the $CD4^+CD25^+$ Isolation Kit II microbeads (Miltenyi Biotec, Auburn, CA). The remaining cells (i.e. non-Treg) were harvested from in a two step procedure. Magnetically labeled non-CD4+ T cells were eluted from a column following the negative selection of CD25-PE labeled CD4+ T cells; subsequently, CD25+ PE-labeled cells in the enriched CD4+ T cell fraction were retained on a column, whilst the unlabeled, non–Treg cells were collected. Non-CD4+ (step1), non-CD25-PE-labeled Treg (step 2) cells were pooled and used in the assays of **Figure 5**.

***In vivo* depletion studies.** Immune cell depletions were done by i.v. injections (0.1 mg/mouse) of anti-CD8 (Lyt 2.43, BioXcell, West Lebanon, NH) and anti-CD4 (GK1.5 BioXcell, West Lebanon, NH) antibodies; anti–natural killer (NK) cells (anti–asialo-GM-1; Cedarlane, Ontario, Canada) and IgG control (ChromPure Rat IgG; Jackson ImmunoResearch, West Grove, PA) at day 7, 10, 12 after tumor implantation and then weekly thereafter.

Statistics. Survival data from the animal studies were analyzed by the log-rank test using GraphPad Prism 5 (GraphPad Software, La Jolla, CA). Two-sample, unequal variance

Student's t-test analysis was applied for *in vitro* data. Statistical significance was determined at the level of $p < 0.05$.

ACKNOWLEDGEMENTS

This work was supported by The Richard M. Schulze Family Foundation, the Mayo Foundation, Cancer Research UK, the National Institute of Health (RO1CA175386-02; CA108961), The University of Minnesota and Mayo Foundation Partnership, Oncolytics Biotech, Calgary, Canada and a grant from Terry and Judith Paul. We thank Toni Higgins for expert secretarial assistance. Conflict of Interest: This work was funded in part by a grant received from Oncolytics Biotech Incorporated.

References

1. Thirukkumaran, CM*, et al.* (2010). Oncolytic viral therapy for prostate cancer: efficacy of reovirus as a biological therapeutic. *Cancer Res* **70**: 2435-2444.
2. Twigger, K*, et al.* (2012). Reovirus exerts potent oncolytic effects in head and neck cancer cell lines that are independent of signalling in the EGFR pathway. *BMC Cancer* **12**: 368.
3. Errington, F*, et al.* (2008). Reovirus activates human dendritic cells to promote innate antitumor immunity. *J Immunol* **180**: 6018-6026.
4. Prestwich, RJ*, et al.* (2009). Immune-mediated antitumor activity of reovirus is required for therapy and is independent of direct viral oncolysis and replication. *Clin Can Res* **15**: 4374-4381.
5. Qiao, J*, et al.* (2008). Cyclophosphamide facilitates antitumor efficacy against subcutaneous tumors following intravenous delivery of reovirus. *Clin Can Res* **14**: 259-269.
6. Kottke, T*, et al.* (2009). Improved systemic delivery of oncolytic reovirus to established tumors using preconditioning with cyclophosphamide-mediated Treg modulation and interleukin-2. *Clin Can Res* **15**: 561-569.
7. Kottke, T*, et al.* (2010). Antiangiogenic cancer therapy combined with oncolytic virotherapy leads to regression of established tumors in mice. *J Clin Invest* **120**: 1551-1560.
8. Prestwich, RJ*, et al.* (2008). Tumor infection by oncolytic reovirus primes adaptive antitumor immunity. *Clin Can Res* **14**: 7358-7366.
9. Comins, C*, et al.* (2010). REO-10: a phase I study of intravenous reovirus and docetaxel in patients with advanced cancer. *Clin Can Res* **16**: 5564-5572.

10. Galanis, E*, et al.* (2012). Phase II trial of intravenous administration of Reolysin((R)) (Reovirus Serotype-3-dearing Strain) in patients with metastatic melanoma. *Mol Ther* **20**: 1998-2003.

11. Harrington, KJ*, et al.* (2010). Two-stage phase I dose-escalation study of intratumoral reovirus type 3 dearing and palliative radiotherapy in patients with advanced cancers. *Clin Can Res* **16**: 3067-3077.

12. Roulstone, V*, et al.* (2014). Phase I trial of cyclophosphamide as an immune modulator for optimizing oncolytic reovirus delivery to solid tumors. *Clin Can Res **21**: 1304-1312.*

13. Vidal, L*, et al.* (2008). A phase I study of intravenous oncolytic reovirus type 3 Dearing in patients with advanced cancer. *Clin Can Res* **14**: 7127-7137.

14. White, CL*, et al.* (2008). Characterization of the adaptive and innate immune response to intravenous oncolytic reovirus (Dearing type 3) during a phase I clinical trial. *Gene Ther* **15**: 911-920.

15. Harrington, KJ, Vile, RG, Melcher, A, Chester, J, and Pandha, HS (2010). Clinical trials with oncolytic reovirus: moving beyond phase I into combinations with standard therapeutics. *Cytokine Growth Factor Rev* **21**: 91-98.

16. Gollamudi, R*, et al.* (2010). Intravenous administration of Reolysin, a live replication competent RNA virus is safe in patients with advanced solid tumors. *Invest New Drugs* **28**: 641-649.

17. Nishimura, H*, et al.* (2001). Autoimmune dilated cardiomyopathy in PD-1 receptor-deficient mice. *Science* **291**: 319-322.

18. Francisco, LM, Sage, PT, and Sharpe, AH (2010). The PD-1 pathway in tolerance and autoimmunity. *Immunol Rev* **236**: 219-242.

19. Probst, HC, McCoy, K, Okazaki, T, Honjo, T, and van den Broek, M (2005). Resting dendritic cells induce peripheral CD8+ T cell tolerance through PD-1 and CTLA-4. *Nat Immunol* **6**: 280-286.

20. Keir, ME, Butte, MJ, Freeman, GJ, and Sharpe, AH (2008). PD-1 and its ligands in tolerance and immunity. *Annu Rev Immunol* **26**: 677-704.

21. Freeman, GJ*, et al.* (2000). Engagement of the PD-1 immunoinhibitory receptor by a novel B7 family member leads to negative regulation of lymphocyte activation. *J Exp Med* **192**: 1027-1034.

22. Ahmadzadeh, M*, et al.* (2009). Tumor antigen-specific CD8 T cells infiltrating the tumor express high levels of PD-1 and are functionally impaired. *Blood* **114**: 1537-1544.

23. Gros, A*, et al.* (2014). PD-1 identifies the patient-specific CD8(+) tumor-reactive repertoire infiltrating human tumors. *J Clin Invest* **124**: 2246-2259.

24. Dong, H*, et al.* (2002). Tumor-associated B7-H1 promotes T-cell apoptosis: a potential mechanism of immune evasion. *Nat Med* **8**: 793-800.

25. Schreiber, RD, Old, LJ, and Smyth, MJ (2011). Cancer immunoediting: integrating immunity's roles in cancer suppression and promotion. *Science* **331**: 1565-1570.

26. McDermott, DF, and Atkins, MB (2013). PD-1 as a potential target in cancer therapy. *Cancer Med* **2**: 662-673.

27. Zou, W, and Chen, L (2008). Inhibitory B7-family molecules in the tumour microenvironment. *Nat Rev Immunol* **8**: 467-477.

28. Naidoo, J, Page, DB, and Wolchok, JD (2014). Immune modulation for cancer therapy. *Br J Cancer* **111**: 2214-2219.

29. Brahmer, JR*, et al.* (2010). Phase I study of single-agent anti-programmed death-1 (MDX-1106) in refractory solid tumors: safety, clinical activity, pharmacodynamics, and immunologic correlates. *J Clin Oncol* **28**: 3167-3175.

30. Brahmer, JR*, et al.* (2012). Safety and activity of anti-PD-L1 antibody in patients with advanced cancer. *N Engl J Med* **366**: 2455-2465.

31. Stanford, MM, Breitbach, CJ, Bell, JC, and McFadden, G (2008). Innate immunity, tumor microenvironment and oncolytic virus therapy: friends or foes? *Curr Opin Mol Ther* **10**: 32-37.

32. Melcher, A, Parato, K, Rooney, CM, and Bell, JC (2011). Thunder and lightning: immunotherapy and oncolytic viruses collide. *Molecular therapy : the journal of the American Society of Gene Therapy* **19**: 1008-1016.

33. Zamarin, D*, et al.* (2014). Localized oncolytic virotherapy overcomes systemic tumor resistance to immune checkpoint blockade immunotherapy. *Sci Transl Med* **6**: 226ra232.

34. Engeland, CE*, et al.* (2014). CTLA-4 and PD-L1 checkpoint blockade enhances oncolytic measles virus therapy. *Mol Ther* **22**: 1949-1959.

35. Sorensen, MR, Holst, PJ, Steffensen, MA, Christensen, JP, and Thomsen, AR (2010). Adenoviral vaccination combined with CD40 stimulation and CTLA-4 blockage can lead to complete tumor regression in a murine melanoma model. *Vaccine* **28**: 6757-6764.

36. Altomonte, J, and Ebert, O (2012). Replicating viral vectors for cancer therapy: strategies to synergize with host immune responses. *Microb Biotechnol* **5**: 251-259.

37. Diaz, RM*, et al.* (2007). Oncolytic immunovirotherapy for melanoma using vesicular stomatitis virus. *Cancer Res* **67**: 2840-2848.

38. Galivo, F*, et al.* (2010). Interference of CD40L-mediated tumor immunotherapy by oncolytic vesicular stomatitis virus. *Hum Gene Ther* **21**: 439-450.

39. Wongthida, P*, et al.* (2010). Type III IFN interleukin-28 mediates the antitumor efficacy of oncolytic virus VSV in immune-competent mouse models of cancer. *Cancer Res* **70**: 4539-4549.

40. Kottke, T*, et al.* (2008). Treg depletion-enhanced IL-2 treatment facilitates therapy of established tumors using systemically delivered oncolytic virus. *Mol Ther* **16**: 1217-1226.

41. Tumeh, PC*, et al.* (2014). PD-1 blockade induces responses by inhibiting adaptive immune resistance. *Nature* **515**: 568-571.

42. Karyampudi, L*, et al.* (2014). Accumulation of memory precursor CD8 T cells in regressing tumors following combination therapy with vaccine and anti-PD-1 antibody. *Cancer Res* **74**: 2974-2985.

FIGURE LEGENDS

Figure 1. Combination therapy of Reovirus with anti-PD-1 antibody. **A.** C57BL/6 mice bearing 7 days established s.c. B16 tumors were treated with three doses of i.t. reovirus ($7x10^8$ pfu/50µl) or with PBS (days 7,10,12). Starting on day 14, mice were treated i.v. with anti-PD-1 antibody (0.25 mg/mouse), or with isotype control IgG (ctl IgG), every other day for 8 injections. Survival of tumor-bearing C57BL/6 mice (*n*=7 mice per group) is shown. Data are representative of two separate experiments. * p = 0.0084, **P = 0.0005

Figure 2. PD-1 blockade enhances i.t. reovirus induced Th1 memory T cell responses. **A.** Splenocytes/LN cells from individual C57BL/6 mice bearing s.c. B16 tumors, and treated with a combination of i.t. PBS or reovirus and i.v. isotype control antibody (control IgG) or anti-PD-1 antibody as labeled, were re-stimulated *in vitro* with freeze-thaw (F/T) lysates of B16 tumor cells (equivalent of 10^6 cells per stimulation). 48hrs later supernatants were assayed for secretion of IFN-ɤ by ELISA. The numbers on the x-axis indicate the mouse number in each treatment group. Error bars represent the standard deviation of measurements from triplicate wells per sample. **B.** Splenocytes/LN from C57BL/6 mice bearing s.c. B16 tumors, and treated with a combination of i.t. reovirus with i.v. control isotype IgG (black bars) or with anti-PD-1 (hatched bars) were re-stimulated *in vitro* with B16 F/T lysates, or with peptides for specific melanoma antigens as shown. 48hrs later, supernatants were assayed for IFN-γ by ELISA. Each bar represents splenocytes/LN from an individual mouse and measurements were made from two mice treated with (i.t. reovirus and i.v. control IgG), or two mice treated with (i.t. reovirus and i.v. anti-PD-1).

Figure 3. PD-1 blockade augments reovirus-induced NK cell activation and killing. B16 cells were mock infected, or infected with reovirus at MOI= 0.1 in the presence of anti-PD-1, anti-PD-L1, or isotype control antibody (ctl IgG) at 100 ng/ml. Forty-eight hours later, cells were incubated with splenic NK cells isolated from tumor naïve mice at E:T 10:1. 4 days post

infection, supernatants were assayed for **A.** TNF-α secretion by ELISA *** p<0.0001 or **B.** for reovirus titers using plaque assays. **C.** 7 days -post-infection surviving cells were counted. **D-F**.Splenocytes from C57Bl/6 mice were stained with CD3-FITC, NK-Pe/Cy7 CD4-Percp, CD8-PE, PD-1-PE/Cy7 fixed and analyzed by flow cytometry. Expression of PD-1 on NK cells **(D)**, CD4 T cells **(E)** and CD8 T cells **(F)** is shown. **G**. Splenic NK cells isolated from tumor naïve mice were stained with CD3-FITC, NK-PE and PD-1 PE/Cy7. Percentages of CD3+ and NK+ cells is shown (left panel). CD3+ cells were further analyzed for PD-1 expression (right panel).

Figure 4. **NK recognition of reovirus-infected B16 cells up-regulates PD-L1 expression A**. B16 tumor cells were mock (red curve) or reovirus infected at MOI-0.1 (blue curve). After four days, the cells were trypsinized, harvested, stained with antibodies against CD45-PerCP, PD-L1-APC, fixed and analyzed by flow cytometry. PD-L1 expression is shown. **B&C.** Co-culture incubation. B16 tumor cells were mock (red curve) or reovirus infected at MOI-0.1 (blue curve). Forty-eight hours post-infection, NK cells were added at E:T 10:1. Co-cultures, and B16 without NK cells (orange curve), were then incubated for a further forty-eight hours. Supernatants were collected and centrifuged to isolate NK cells, and tumor cells were trypsinized and harvested. Tumor cells were stained with antibodies against CD45-PerCP, PD-L1-APC, fixed and analyzed by flow cytometry; PD-L1 expression is shown (panel B). NK cells were stained with antibodies against CD3-FITC, NK1.1-PE, PD-L1-APC, fixed and analyzed using flow cytometry; PD-L1 expression is shown (panel C).

Figure 5. PD-1 blockade ablates tumor-specific immune suppression by T_{reg}. A. C57BL/6 mice bearing s.c. B16 tumors were treated with i.t. reovirus, in combination with i.v. anti-PD-1 or isotype (control) IgG (2 mice per group). Non-depleted splenocytes/LN cells (black bars), or splenocytes/LN depleted for $CD8^+$ T cells (white bars) or T_{reg} (hatched bars) were stimulated *in vitro* with **A.** F/T lysates of B16. Forty-eight later supernatants were assayed for IFN-ɤ by

ELISA. Values represent levels each done in triplicate wells (mean ± standard deviation). **B.** Splenocytes/LN from C57BL/6 mice treated with i.t. reovirus, in combination with i.v. anti-PD-1, isotype (control) IgG, or PBS (4 mice per group) were stimulated with F/T lysates of reovirus-infected TC2 cells. 48hrs later, supernatants were assayed for IFN-ɣ by ELISA. Values represent secretion levels for three or four different mice per group, each done in triplicate wells (means ± standard deviation). **C.** C57BL/6 mice bearing s.c. B16 tumors were treated with i.t. PBS or reovirus, in combination with i.v. anti-PD-1 or isotype (control) IgG. Non-depleted splenocytes/LN cells (black bars), or splenocytes/LN depleted for $CD8^+$ T cells (white bars) or T_{reg} (hatched bars) were stimulated *in vitro* with F/T lysates of reovirus-infected TC2 cells, * ($p< 0.0001$). **D**. C57BL/6 mice bearing s.c. B16 tumors were treated with i.t. PBS or reovirus, with four doses of i.v. anti-PD-1 or isotype (control) IgG. On day 22 after tumor implant, tumors were harvested and stained for CD45-PerCP, CD4-FITC, CD25-Pe/Cy7 followed by intracellular staining with Foxp3-PE or with CD45-PerCP, CD8-PE. The percentages of tumor-infiltrating CD3+ T cells which are T_{regs} (left panel) or CD8+ T cells (right panel) are shown. Six tumors were analyzed from each treatment group with mean and standard deviation shown.

Figure 6. Combination therapy of reovirus and anti-PD-1 antibody is dependent upon NK cells and CD8+ T cells. **A.** 7 days post s.c. B16 tumor challenge, reovirus or PBS were administered i.t. along with i.v. injections of depleting antibodies against CD8+ T cells, CD4+ T cells or NK cells at days 7,10 and 12 and weekly thereafter. At days 14,17,19,26,28,30,32, and 33 anti-PD-1 or PBS were administered via i.v injections. Survival of tumor-bearing C57BL/6 mice (*n*=7 mice per group) is shown. * $p = 0.0024$, ** $p= 0.0004$

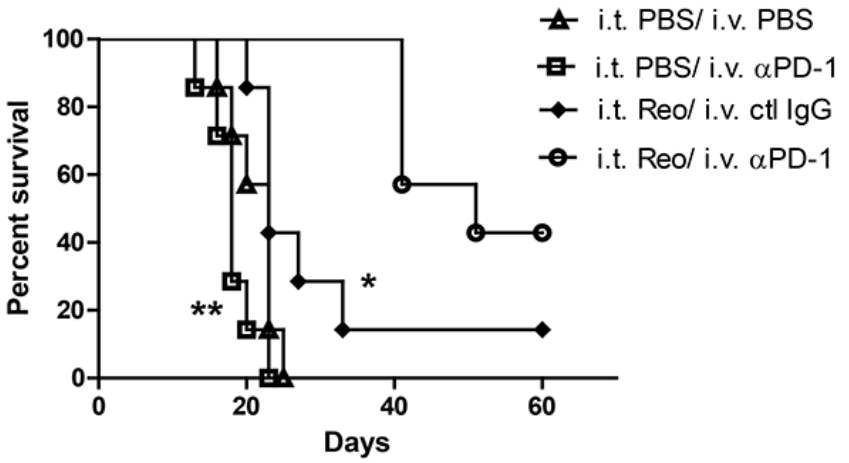

Figure 1

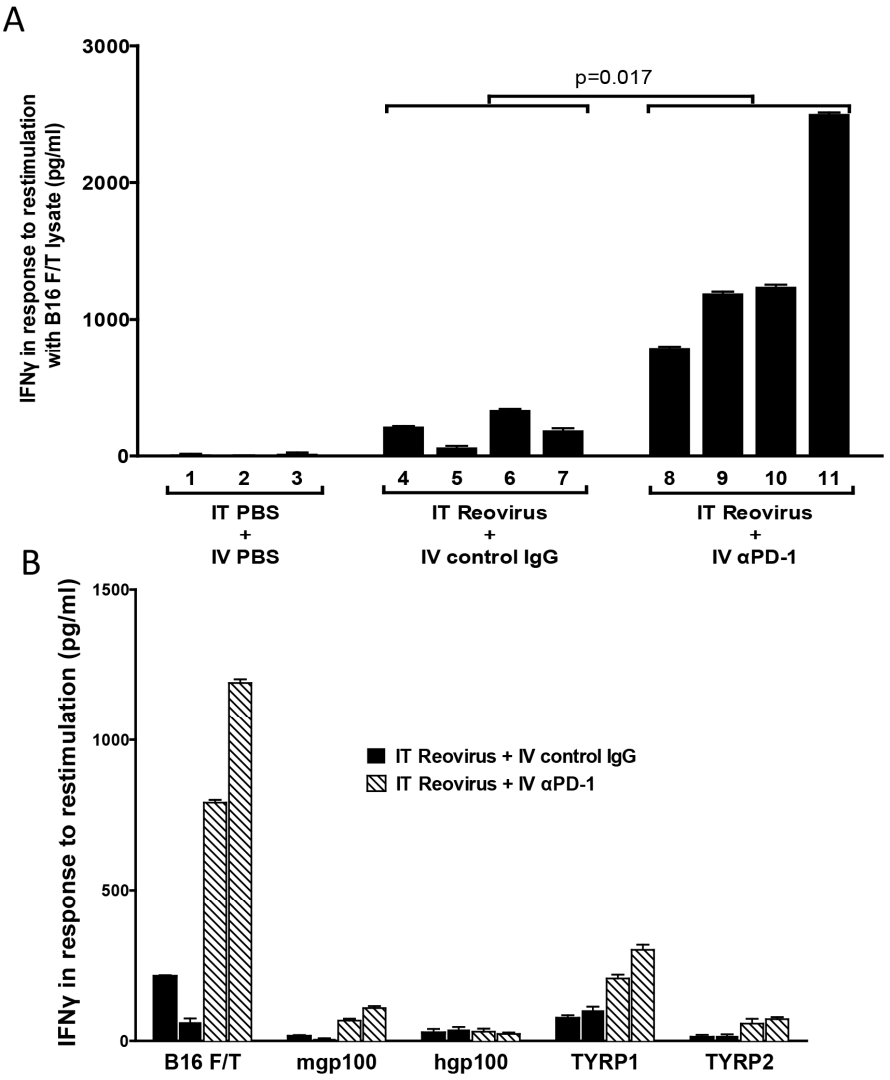

Figure 2

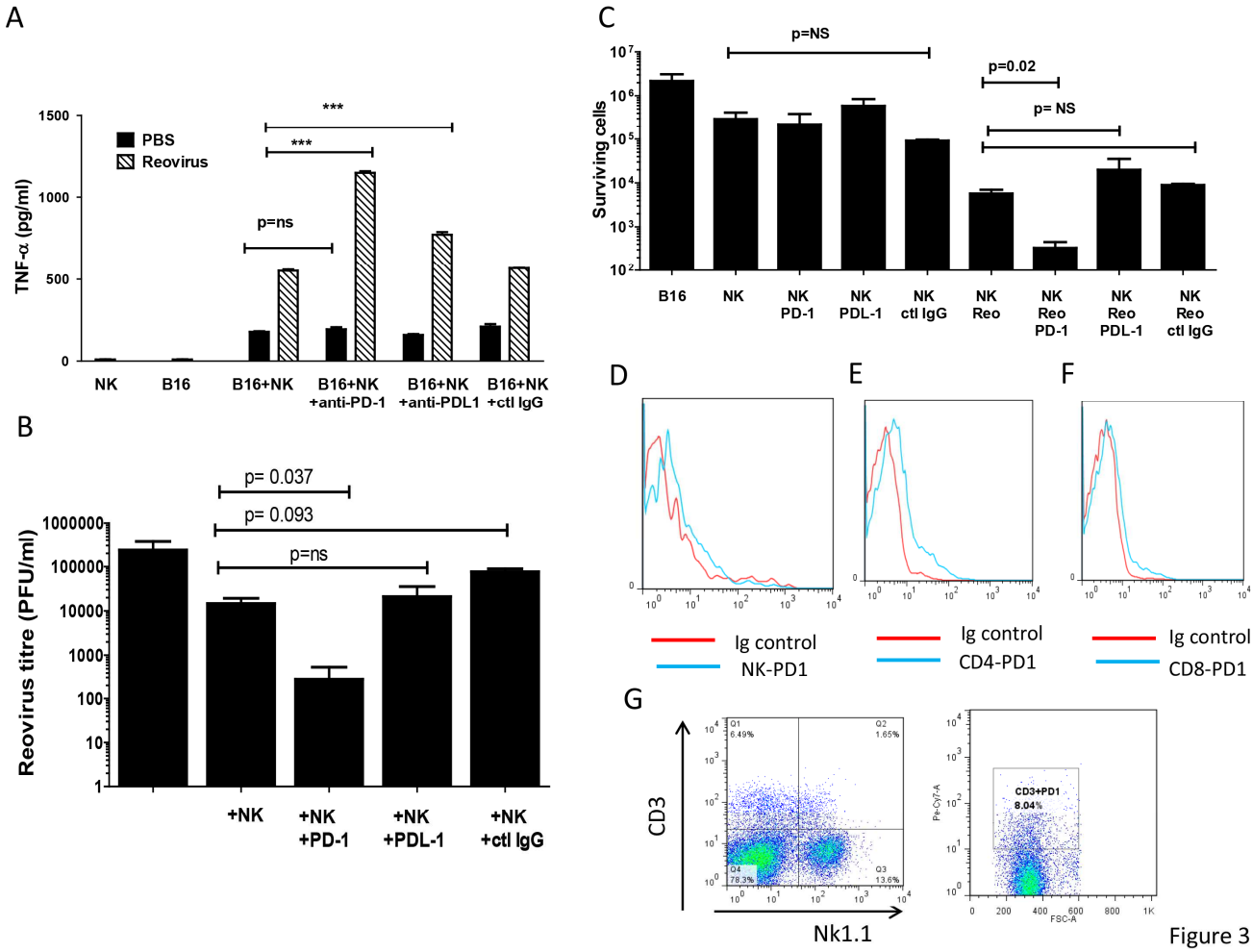

Figure 3

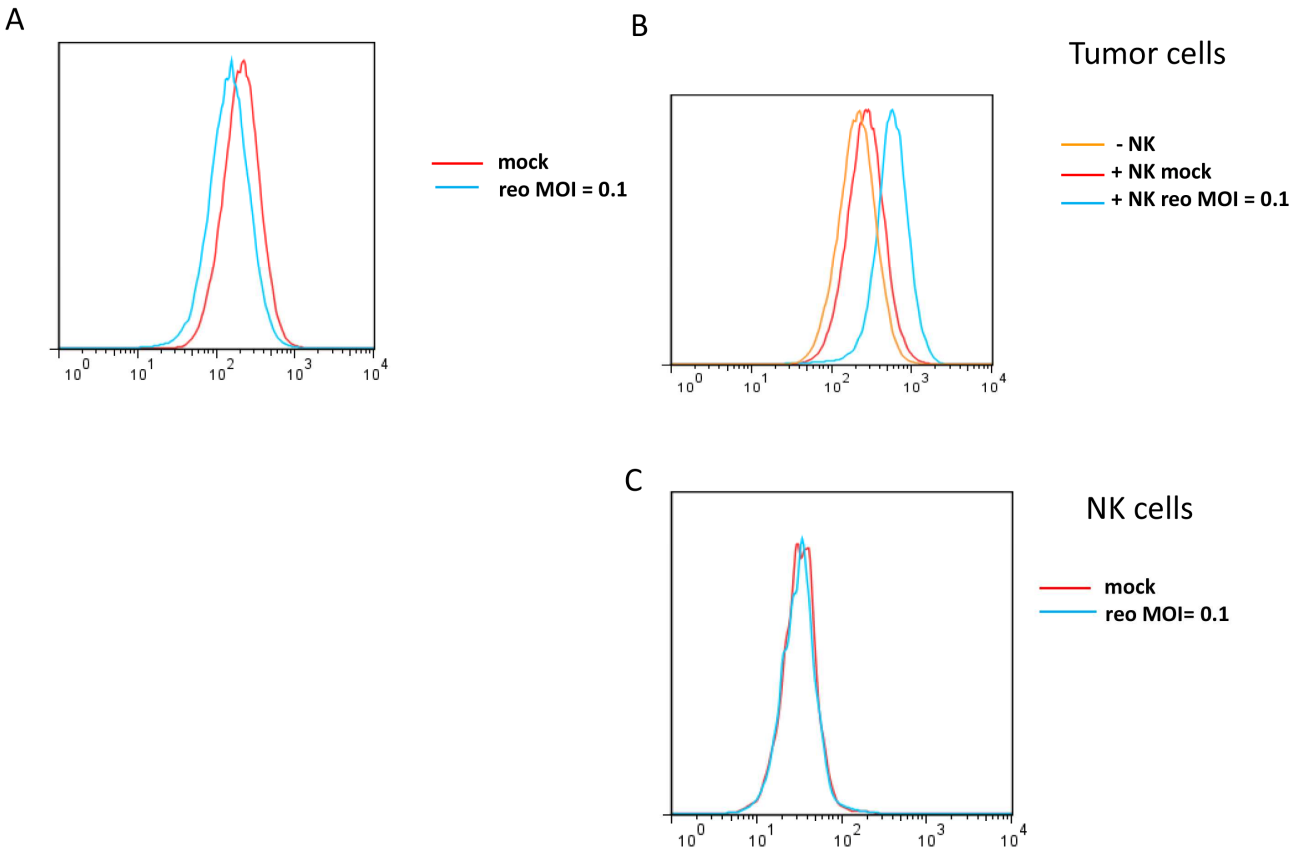

Figure 4

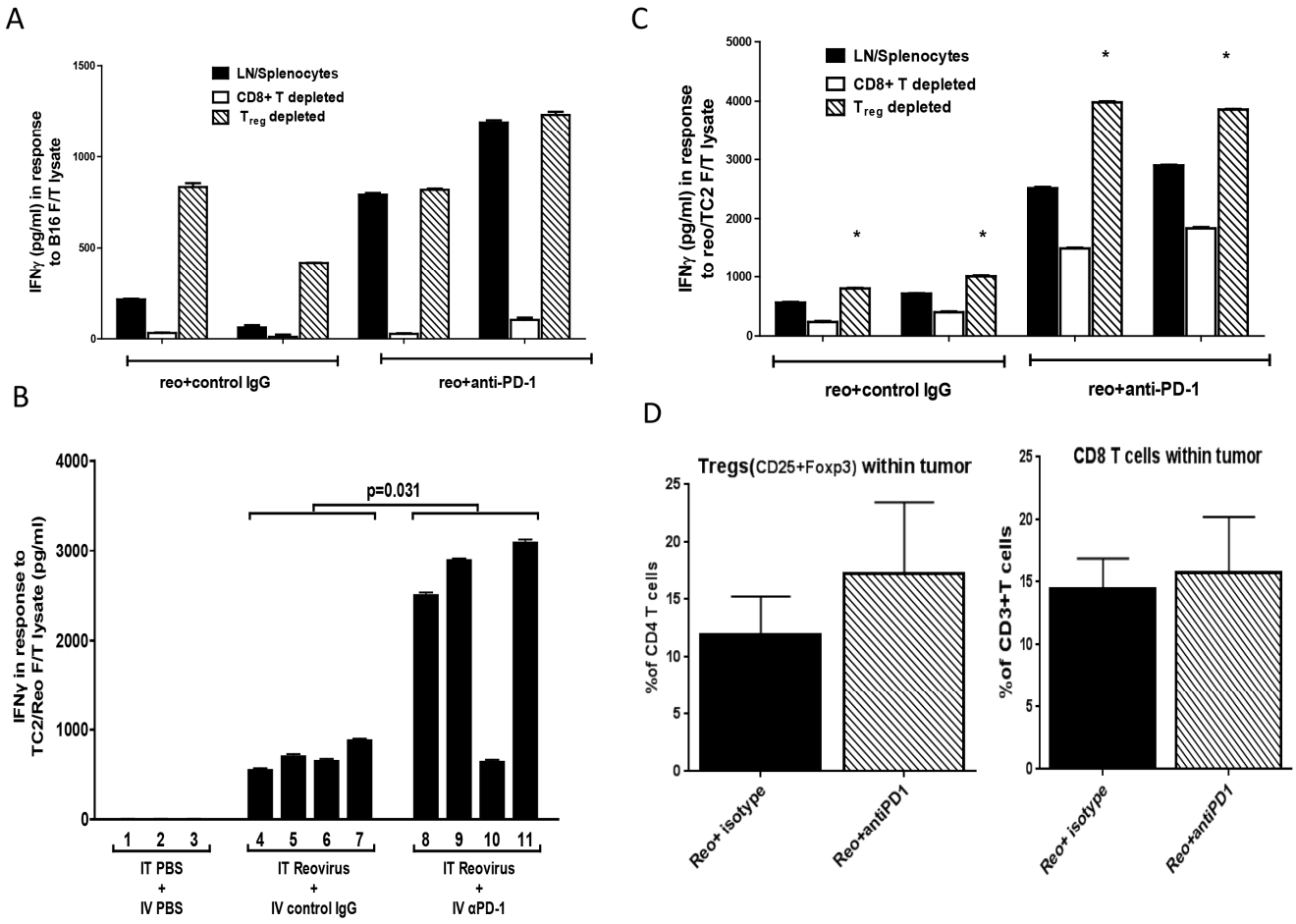

Figure 5

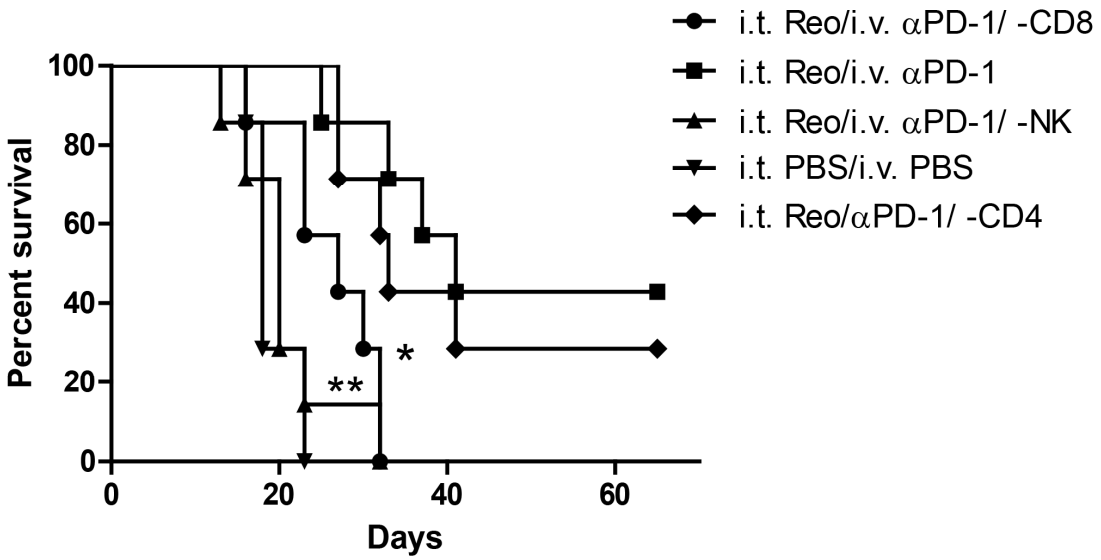

Figure 6